A Cooperative Control Approach for Multi-quadrotor Formation in Agricultural Scenarios with Obstacles and External Disturbances

Pablo Raul Yanyachi, *Senior Member, IEEE,* Luis F. Canaza Ccari, and Daniel D. Yanyachi

***Abstract*—This research aims to develop a robust cooperative control approach for the flight formation of multiple quadrotors in trajectory tracking tasks in agricultural scenarios with obstacles and external disturbances. For this purpose, a distributed autonomous control framework is proposed that integrates a guidance system and an advanced control system for each quadrotor under a leader-follower control scheme. The guidance system employs the Artificial Potential Field (APF) algorithm, which guarantees attraction to the target while avoiding obstacles. For the control system, a distributed consensus protocol based on an Adaptive Integral Fast Terminal Sliding Mode Control (AIFTSMC) is implemented, ensuring fast convergence and robust tracking of the reference trajectory, maintaining the alignment of the quadrotors throughout the entire flight mission. The validity of the proposed approach has been demonstrated through numerical simulations performed in MATLAB/Simulink, implementing a representative agricultural scenario. The results show that the approach offers robust and efficient performance for multiple quadrotor flight formation in agricultural environments, even in the presence of external disturbances and obstacles.**

Link to graphical and video abstracts, and to code: https://latamt.ieeer9.org/index.php/transactions/article/view/9413

***Index Terms*—quadrotor, Multi-UAV, Formation control, Adaptive control.**

I. Introduction

In recent years, cooperative formation control of multiple quadrotor has attracted a great deal of interest in the research community, especially in the field of aerospace engineering. This is due to the numerous applications that multi-quadrotor systems can have in various industries and sectors, such as cooperative transportation of construction materials [1], search and rescue missions [2], and precision agriculture [3].

In the field of precision agriculture, multiple quadrotors can be used to perform various agricultural tasks, such as crop monitoring, mapping, spraying, and irrigation, among others [4], [5]. In this context, using multiple quadrotors for such tasks would allow efficiently addressing large areas of land in reduced periods of time, improving operational efficiency compared to using a single quadrotor [6], [7]. However, for these applications to be feasible, advanced control systems must be developed to enable precise planning and optimal trajectory tracking quadrotor control is challenging due to the underactuated nature of these aircraft, which have six degrees of freedom and only four control inputs, as well as possessing complex and highly coupled nonlinear dynamics [8]–[10].

Several advanced control strategies have been proposed in the literature for quadrotors in agricultural applications. For example, in [11], an adaptive sliding mode control algorithm based on neural networks was developed for agricultural trajectory tracking. In [12], a controller based on type-2 fuzzy neural networks and a hybrid particle swarm optimization algorithm for autonomous crop inspection was presented. More recently, in [13], an adaptive sliding mode control was proposed for position dynamics, complemented by a fast terminal sliding control for attitude dynamics. However, these works [11]–[13] focused only on a single quadrotor, limiting their applicability in large-scale agricultural scenarios. Although farmers tend to employ a single quadrotor nowadays, this approach has distinct limitations, such as limited flight time, reduced coverage, and low payload capacity [14].

Given this, the need arises to employ multiple quadrotors to overcome these limitations and maximize the potential of precision agriculture. However, controlling multiple quadrotors simultaneously adds considerable complexity due to trajectory planning, the risk of collisions, and the complex nature of these vehicles' dynamics [15]–[17].

In this context, the literature has attempted to address these issues, although work on advanced control of multiple quadrotors in precision agriculture applications still needs to be explored and continues to be an active research topic. For example, in [18], a distributed control law based on sliding mode control theory was proposed for the formation of three agricultural quadrotors. However, this approach employed a linear (conventional) sliding surface, which causes the phenomenon known as chattering, which can damage aircraft engines in practical applications. In [19], cooperative transport of loads by multiple quadrotors was studied in the context of agricultural spraying applications, using a PID approach for distance-based formation control. Similarly, in [20], a distributed PID control system for a set of quadrotors was developed using a swarm algorithm. It is relevant to note that the latter work [20] performed an experimental performance comparison between the use of a single quadrotor, which is most common today, and the use of three quadrotors,

The associate editor coordinating the review of this manuscript and approving it for publication was Roberto S. Murphy (*Corresponding author: Pablo Raul Yanyachi*).

Pablo Raul Yanyachi, L. F. C. Canaza, and D. Yanyachi are with the Instituto de Investigación Astronómico y Aeroespacial Pedro Paulet, Universidad Nacional de San Agustín de Arequipa, Arequipa, Perú (e-mails: raulpab@unsa.edu.pe, lcanazacc@unsa.edu.pe, and dyanyachi@unsa.edu.pe).

confirming the superiority of the cooperative approach in agricultural applications. Despite the advances in these studies [19], [20], both employed classical PID control laws, which, although widely used in the literature, do not provide adequate robustness against large external disturbances, as demonstrated in the experimental study in [21]. Moreover, those works did not consider the presence of obstacles in path planning, despite the fact that the occurrence of obstacles is common in agricultural scenarios. This highlights the need to integrate effective guidance algorithms that ensure obstacle avoidance within the control system.

In summary, although several advanced control strategies for quadrotors in agricultural scenarios have been proposed in previous works [11]–[13], these studies have focused on controlling a single vehicle. On the other hand, the works that address the use of multiple quadrotors [18]–[20] employ classical controllers that do not offer sufficient robustness to large disturbances and also do not consider the presence of obstacles in the trajectory planning. Given this situation, this research proposes developing a distributed autonomous control framework for the formation of multiple quadrotors with the ability to follow trajectories in agricultural environments that include obstacles and external disturbances. This framework integrates a guidance system for trajectory planning and an advanced control system that ensures robust and reliable tracking of the desired formation trajectory, thus optimizing performance in this type of application. The scope of this article is limited to showing verification results of the mathematics in MATLAB/Simulink software of the proposed algorithm and control law.

A. Contributions

The main contributions of this research are as follows:

- Unlike the formation control approaches presented in [18]–[20], this research proposes a distributed autonomous control framework that integrates a guidance system and an advanced control system. The guidance system uses the Artificial Potential Field (APF) algorithm, while the control system is based on a distributed consensus protocol implemented using the Adaptive Integral Fast Terminal Sliding Mode Control Strategy (AIFTSMC).
- The AIFTSMC control strategy guarantees finite-time stability, which allows a fast convergence of the quadrotors to the reference trajectory. In addition, the adaptive laws integrated in this strategy ensure robust trajectory planning and tracking, even in the presence of obstacles and external disturbances.
- Simulations were carried out in the MATLAB/Simulink environment, in which a typical agricultural scenario was implemented with the presence of obstacles and external disturbances. The results demonstrated that the proposed guidance and control framework provides robust and efficient performance in multiple quadrotor flight formation in agricultural environments.

The rest of the paper is organized as follows: Section III presents the problem statement, including the dynamic model of the multi-quadrotor system and the objective of the research. Section IV discusses the development of the proposed guidance and control system, along with the stability analysis. Section V presents the results obtained, and finally, Section VI discusses the conclusions of the research.

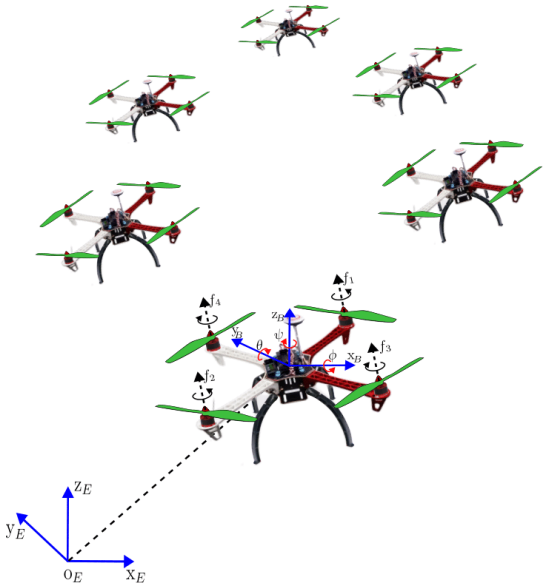

Fig. 1. Flight formation of a multi-quadrotor system [22].

II. Preliminaries

A. Graph Theory

Consider a collection of N quadrotor agents that interact with their neighbors, represented by the graph $G = (V, E)$, where V represents the vertices and E denotes the edges. An edge (V_i, V_j) implies that quadrotor agent i can access the information of quadrotor agent j and vice versa. The adjacency matrix of the graph is denoted by A, with elements $a_{ij} > 0$ if $(V_i, V_j) \in E$ and $a_{ij} = 0$ otherwise. The degree matrix is defined as $D = \text{diag}(d_1, ..., d_N) \in \mathbb{R}^{N\times N}$, where $d_i = \sum_{j=1}^{N} a_{ij}$. Therefore, the Laplacian matrix can be expressed as $L = D - A$. Consider a diagonal matrix $B = \text{diag}(b_1, ..., b_N)$ that represents the data flow interconnection from the leader to the followers, where $b_i > 0$ if the leader agent sends its information to the follower agent i; otherwise, $b_i = 0$.

B. Lemmas

Lemma 1: [25] For any Lyapunov function that verifies the following inequality $\dot{V}(x) \leq -\varpi_1 V - \varpi_2 V^{\Pi}$, where the constants $\varpi_1 > 0, \varpi_2 > 0, 0 < \Pi < 1$, there exists a finite time stability so that the settling time is given by:

$$T_f \leq \frac{1}{(1-\Pi)\varpi_1} \ln\left(\frac{\varpi_1 V^{1-\Pi}(x(0)) + \varpi_2}{\varpi_2}\right)$$

.

III. Problem Statement

A. Dynamic model of the multi-quadrotor system

Consider a multi-agent system composed of N quadrotors, as shown in Fig. 1, where it is assumed that each quadrotor follows the same dynamic model. The motion of the i-th quadrotor in space can be decomposed into translational and rotational movements. Each aerial vehicle is associated with two coordinate frames: one body-fixed and one earth-fixed (see Fig. 1). Therefore, the dynamic model of the i-th quadrotor is described as follows [22]:

$$\begin{cases} \ddot{x}_i = m_i^{-1}\left[(c\phi_i s\theta_i c\psi_i + s\phi_i s\psi_i)u_{i,z} - \bar{k}_{i,x}\dot{x}_i + d_{i,x}^{ext}\right], \\ \ddot{y}_i = m_i^{-1}\left[(c\phi_i s\theta_i s\psi_i - s\phi_i c\psi_i)u_{i,z} - \bar{k}_{i,y}\dot{y}_i + d_{i,y}^{ext}\right], \\ \ddot{z}_i = m_i^{-1}\left[(c\phi_i c\theta_i)u_{i,z} - \bar{k}_{i,z}\dot{z}_i + d_{i,z}^{ext}\right] - g, \\ \ddot{\phi}_i = J_{i,x}^{-1}\left[(J_{i,y}-J_{i,z})\dot{\theta}_i\dot{\psi}_i - J_{i,r}\dot{\theta}_i\overline{\omega}_i - \bar{k}_{i,\phi}\dot{\phi}_i^2 + u_{i,\phi} + d_{i,\phi}^{ext}\right], \\ \ddot{\theta}_i = J_{i,y}^{-1}\left[(J_{i,z}-J_{i,x})\dot{\phi}_i\dot{\psi}_i + J_{i,r}\dot{\phi}_i\overline{\omega}_i - \bar{k}_{i,\theta}\dot{\theta}_i^2 + u_{i,\theta} + d_{i,\theta}^{ext}\right], \\ \ddot{\psi}_i = J_{i,z}^{-1}\left[(J_{i,x}-J_{i,y})\dot{\phi}_i\dot{\theta}_i - \bar{k}_{i,\psi}\dot{\psi}_i^2 + u_{i,\psi} + d_{i,\psi}^{ext}\right], \end{cases} \tag{1}$$

where $\xi_i = [x_i, y_i, z_i]^T$ and $v_i = [\dot{x}_i, \dot{y}_i, \dot{z}_i]^T$ represent the position and linear velocity of the i-th quadrotor, respectively, while m_i denotes its mass, and g is the acceleration due to gravity. The scalar $u_{i,z}$ corresponds to the total thrust force generated by the four rotors, and $\bar{k}_{i,x}, \bar{k}_{i,y}, \bar{k}_{i,z}$ are the translational aerodynamic drag coefficients. Additionally, $\eta_i = [\phi_i, \theta_i, \psi_i]^T$, $\omega_i = [\dot{\phi}_i, \dot{\theta}_i, \dot{\psi}_i]^T$, and $J_i = \text{diag}(J_{i,x}, J_{i,y}, J_{i,z})$ represent the orientation, angular velocity, and moment of inertia of the i-th quadrotor, respectively. The vector $\tau_{i,m} = [u_{i,\phi}, u_{i,\theta}, u_{i,\psi}]^T$ denotes the torques generated by the motors, while $J_{i,r}$ represents the rotor inertia. The coefficients $\bar{k}_{i,\phi}, \bar{k}_{i,\theta}, \bar{k}_{i,\psi}$ correspond to the aerodynamic friction coefficients for rotational motion. Finally, $d_{i,\xi}^{ext} = [d_{i,x}^{ext}, d_{i,y}^{ext}, d_{i,z}^{ext}]$ and $d_{i,\eta}^{ext} = [d_{i,\phi}^{ext}, d_{i,\theta}^{ext}, d_{i,\psi}^{ext}]$ represent the external disturbances acting on the translational and rotational dynamics, respectively.

The thrust force $u_{i,z}$ and the motor torques $u_{i,\phi}, u_{i,\theta}, u_{i,\psi}$ serve as the control inputs for the quadrotor. These control inputs are generated by the aircraft's actuators and are determined based on the angular velocities of the quadrotor's four rotors, as follows [23]:

$$\begin{bmatrix} u_{i,z} \\ u_{i,\phi} \\ u_{i,\theta} \\ u_{i,\psi} \end{bmatrix} = \begin{bmatrix} \kappa_t & \kappa_t & \kappa_t & \kappa_t \\ -\kappa_t l & \kappa_t l & \kappa_t l & -\kappa_t l \\ \kappa_t l & -\kappa_t l & \kappa_t l & -\kappa_t l \\ -\kappa_d & -\kappa_d & \kappa_d & \kappa_d \end{bmatrix} \begin{bmatrix} \Omega_1 \\ \Omega_2 \\ \Omega_3 \\ \Omega_4 \end{bmatrix}, \tag{2}$$

where κ_t is the thrust coefficient, κ_d denotes the drag coefficient, and l represents the distance between the centre of mass of the i-th quadrotor and the rotors.

Based on the dynamics of the i-th quadrotor, presented in (1), it can be observed that the system has six controlled outputs $(x_i, y_i, z_i, \phi_i, \theta_i, \psi_i)$ but only four control inputs $(u_{i,z}, u_{i,\phi}, u_{i,\theta}, u_{i,\psi})$. For this reason, quadrotors are considered complex underactuated systems. To address the underactuation problem, the following virtual control inputs are introduced:

$$\begin{bmatrix} f_{i,x} \\ f_{i,y} \\ f_{i,z} \end{bmatrix} = \begin{bmatrix} m_i^{-1}(c\phi_i s\theta_i c\psi_i + s\phi_i s\psi_i)u_{i,z} \\ m_i^{-1}(c\phi_i s\theta_i s\psi_i - s\phi_i c\psi_i)u_{i,z} \\ m_i^{-1}(c\phi_i c\theta_i)u_{i,z} - g \end{bmatrix}. \tag{3}$$

Now, the total thrust force $u_{i,z}$ and the desired attitude angles (ϕ_i^d, θ_i^d) are defined as a function of the virtual forces $(f_{i,x}, f_{i,y}, f_{i,z})$ as follows:

$$\begin{cases} u_{i,z} = m_i\sqrt{(f_{i,x})^2 + (f_{i,y})^2 + (f_{i,z}+g)^2}, \\ \phi_i^d = \text{asin}\left[\dfrac{m_i}{u_{i,z}}\left(f_{i,x}\sin\psi_i^d - f_{i,y}\cos\psi_i^d\right)\right], \\ \theta_i^d = \text{atan}\left[\dfrac{1}{f_{i,z}+g}\left(f_{i,x}\cos\psi_i^d + f_{i,y}\sin\psi_i^d\right)\right]. \end{cases} \tag{4}$$

B. Control Objective

The objective of this research is to develop a robust cooperative control approach for the flight formation of multiple quadrotors during trajectory tracking tasks in agricultural scenarios, accounting for the presence of obstacles and external disturbances. To achieve this goal, the formation control system must satisfy the following requirements:

- The quadrotors must achieve the desired formation pattern in a short time while avoiding obstacles and maintaining their alignment throughout the entire flight mission.
- The formation tracking errors must converge to zero in a finite time and remain in the vicinity of the origin, i.e.:

$$\begin{cases} \lim\limits_{t\to t_f}(\xi_i - \xi_j) \to (\delta_{ij}^{\xi}), \\ \lim\limits_{t\to t_f}(\xi_i - \xi_0) \to (\delta_{i0}^{\xi}), \end{cases} \tag{5}$$

  where $\delta_{ij}^{\xi} = [\delta_{ij}^x, \delta_{ij}^y, \delta_{ij}^z]^T \in \mathbb{R}^3$ represents the desired position deviation between the i-th aircraft and the j-th aircraft that determines the desired formation pattern.
- The formation control system must ensure adaptability to enable precise planning and robust tracking of the reference trajectory.

IV. Design of the Guidance and Control System

This section describes the development of the distributed autonomous control framework for the formation control of multiple quadrotors in agricultural environments. First, the guidance system is introduced based on the Artificial Potential Field (APF) algorithm for optimal path planning and efficient obstacle avoidance for each quadrotor. Next, the control system is described. The flight controller of each quadrotor is divided into a position controller and an attitude controller. A distributed consensus protocol is implemented based on an Adaptive Integral Fast Terminal Sliding Mode Control (AIFTSMC), which ensures fast convergence and robust tracking of the reference trajectories. Finally, the closed-loop stability of the system is demonstrated using Lyapunov's theory. The development of each stage is detailed below:

A. Guidance System

In this paper, we employ the Artificial Potential Field (APF) algorithm for quadrotor trajectory planning. While simple yet efficient, this algorithm simulates virtual forces and is widely used for obstacle avoidance in robotic systems [24]. In this technique, two potential fields are modeled: the attractive potential field, which aims to guide the UAV toward the target, and the repulsive potential field, which aims to avoid obstacles and prevent collisions. The model for each of these fields is explained below.

1) Attractive Potential Field: Let $\xi = [x, y, z]^T$ be the current position of the quadrotor, and $\xi_d = [x_d, y_d, z_d]^T$ be the reference position. Therefore, the attractive potential field can be expressed as:

$$\Gamma_{\mathrm{a}}(\xi) = \frac{1}{2} k_a \Xi(\xi, \xi_d)^2. \tag{6}$$

where $\Xi(\xi, \xi_d) = \|\xi - \xi_d\|$ denotes the Euclidean distance between the quadrotor's current position and the reference position, and k_a is a positive-defined attraction constant.

The attractive force $F_{\mathrm{a}}(\xi_i)$ of the quadrotor can be defined as the negative gradient of (6):

$$F_{\mathrm{a}}(\xi_i) = -\nabla \Gamma_{\mathrm{a}}(\xi_i) = -k_a \Xi(\xi, \xi_d). \tag{7}$$

2) Repulsive Potential Field: Let $\chi_{\mathrm{obs}} = [x_{\mathrm{obs}}, y_{\mathrm{obs}}, z_{\mathrm{obs}}]^T$ represent the position coordinates of an obstacle; the repulsive potential field can be expressed as:

$$\Gamma_{\mathrm{r}}(\xi_i) = \begin{cases} \frac{1}{2} k_r \left(\frac{1}{\Pi(\xi)} - \frac{1}{\Pi_{\mathrm{obs}}} \right)^2 & \text{if } \Pi(\xi) \le \Pi_0 \\ 0 & \text{if } \Pi(\xi) > \Pi_0, \end{cases} \tag{8}$$

where $\Pi(\xi) = \|\xi - \chi_{\mathrm{obs}}\|$ denotes the Euclidean distance between the quadrotor and the obstacle, Π_{obs} denotes the obstacle's influence distance, and k_r is a positive-defined repulsion constant.

The repulsive force $F_{\mathrm{r}}(\xi)$ of the quadrotor can be defined as the negative gradient of (8):

$$\begin{aligned} F_{\mathrm{r}}(\xi) &= -\nabla \Gamma_{\mathrm{r}}(\xi_i) \\ &= \begin{cases} k_r \left(\frac{1}{\Pi(\xi)} - \frac{1}{\Pi_{\mathrm{obs}}} \right) \frac{1}{\Pi(\xi)^3} \Xi(\xi, \xi_d) & \text{if } \Pi(\xi) \le \Pi_{\mathrm{obs}} \\ 0 & \text{if } \Pi(\xi) > \Pi_{\mathrm{obs}}. \end{cases} \end{aligned} \tag{9}$$

Finally, the total force acting on each quadrotor is the sum of the attractive and repulsive forces, as follows:

$$F_T = F_{\mathrm{a}}(\xi) + \sum_{\kappa=1}^{n} F_{\mathrm{r}}^{\kappa}(\xi), \tag{10}$$

where n is the number of obstacles in the flight scenario.

B. Control System

1) Position control: In this subsection, we design the virtual control inputs $(f_{i,x}, f_{i,y}, f_{i,z})$ for the translational dynamics control of the i-th quadrotor. To do this, we first define the formation tracking errors as:

$$\begin{bmatrix} e_{i,x} \\ e_{i,y} \\ e_{i,z} \end{bmatrix} = \begin{bmatrix} \sum_{j=1}^{N} a_{ij}(x_i - x_j - \delta_{ij}^x) + b_i(x_i - x_0 - \delta_{i0}^x) \\ \sum_{j=1}^{N} a_{ij}(y_i - y_j - \delta_{ij}^y) + b_i(y_i - y_0 - \delta_{i0}^y) \\ \sum_{j=1}^{N} a_{ij}(z_i - z_j - \delta_{ij}^z) + b_i(z_i - z_0 - \delta_{i0}^z) \end{bmatrix} \tag{11}$$

where ξ_i and ξ_0 represent the position of the i-th quadrotor and the leader of the group, respectively. The term $\delta_{ij}^{\xi} = [\delta_{ij}^x, \delta_{ij}^y, \delta_{ij}^z]^T \in \mathbb{R}^3$ denotes the desired position deviation between the i-th agent and the j-th agent.

By taking the time derivative of the formation tracking errors (11), we have:

$$\begin{bmatrix} \dot{e}_{i,x} \\ \dot{e}_{i,y} \\ \dot{e}_{i,z} \end{bmatrix} = \begin{bmatrix} \sum_{j=1}^{N} a_{ij}(\dot{x}_i - \dot{x}_j) + b_i(\dot{x}_i - \dot{x}_0) \\ \sum_{j=1}^{N} a_{ij}(\dot{y}_i - \dot{y}_j) + b_i(\dot{y}_i - \dot{y}_0) \\ \sum_{j=1}^{N} a_{ij}(\dot{z}_i - \dot{z}_j) + b_i(\dot{z}_i - \dot{z}_0) \end{bmatrix} \tag{12}$$

The objective is to ensure that the tracking errors converge to zero; therefore, we propose the following integral sliding surface, defined as:

$$\begin{bmatrix} s_{i,x} \\ s_{i,y} \\ s_{i,z} \end{bmatrix} = \begin{bmatrix} c_{1x}\dot{e}_{i,x} + c_{2x}e_{i,x} + c_{3x}\int_0^t [|e_{i,x}|^{\alpha_x}\mathrm{sgn}(e_{i,x})]dt \\ c_{1y}\dot{e}_{i,y} + c_{2y}e_{i,y} + c_{3y}\int_0^t [|e_{i,y}|^{\alpha_y}\mathrm{sgn}(e_{i,y})]dt \\ c_{1z}\dot{e}_{i,z} + c_{2z}e_{i,z} + c_{3z}\int_0^t [|e_{i,z}|^{\alpha_z}\mathrm{sgn}(e_{i,z})]dt \end{bmatrix} \tag{13}$$

where $c_{1\kappa}, c_{2\kappa}, c_{3\kappa}$ for $\kappa = (x, y, z)$ are positive constants representing the controller parameters. The exponents $\alpha_x, \alpha_y, \alpha_z$ satisfy $0 < \alpha_\kappa < 1$ for $\kappa = (x, y, z)$. Taking the time derivative of the sliding surfaces gives:

$$\begin{aligned} \begin{bmatrix} \dot{s}_{i,x} \\ \dot{s}_{i,y} \\ \dot{s}_{i,z} \end{bmatrix} &= \begin{bmatrix} c_{1x}\ddot{e}_{i,x} + c_{2x}\dot{e}_{i,x} + c_{3x}|e_{i,x}|^{\alpha_x}\mathrm{sgn}(e_{i,x}) \\ c_{1y}\ddot{e}_{i,y} + c_{2y}\dot{e}_{i,y} + c_{3y}|e_{i,y}|^{\alpha_y}\mathrm{sgn}(e_{i,y}) \\ c_{1z}\ddot{e}_{i,z} + c_{2z}\dot{e}_{i,z} + c_{3z}|e_{i,z}|^{\alpha_z}\mathrm{sgn}(e_{i,z}) \end{bmatrix} \\ &= \begin{bmatrix} c_{1x}(\sum_{j=1}^{N} a_{ij}(\ddot{x}_i - \ddot{x}_j) + b_i(\ddot{x}_i - \ddot{x}_0)) + \\ c_{2x}\dot{e}_{i,x} + c_{3x}|e_{i,x}|^{\alpha_x}\mathrm{sgn}(e_{i,x}) \\ c_{1y}(\sum_{j=1}^{N} a_{ij}(\ddot{y}_i - \ddot{y}_j) + b_i(\ddot{y}_i - \ddot{y}_0)) + \\ c_{2y}\dot{e}_{i,y} + c_{3y}|e_{i,y}|^{\alpha_y}\mathrm{sgn}(e_{i,y}) \\ c_{1z}(\sum_{j=1}^{N} a_{ij}(\ddot{z}_i - \ddot{z}_j) + b_i(\ddot{z}_i - \ddot{z}_0)) + \\ c_{2z}\dot{e}_{i,z} + c_{3z}|e_{i,z}|^{\alpha_z}\mathrm{sgn}(e_{i,z}) \end{bmatrix} \end{aligned} \tag{14}$$

By enforcing the sliding mode condition $\dot{s}_{i,x} = \dot{s}_{i,y} = \dot{s}_{i,z} = 0$, the equivalent control law is designed as follows:

$$\begin{bmatrix} u_{i,x}^{\mathrm{eq}} \\ u_{i,y}^{\mathrm{eq}} \\ u_{i,z}^{\mathrm{eq}} \end{bmatrix} = \begin{bmatrix} \frac{1}{c_{1x}(\sum_{j=1}^{N} a_{ij} + b_i)} \Big(c_{1x}(\sum_{j=1}^{N} a_{ij}\ddot{x}_j + b_i\ddot{x}_0) + \\ c_{1x}(\sum_{j=1}^{N} a_{ij} + b_i)\bar{k}_{i,x}\dot{x}_i - c_{2x}\dot{e}_{i,x} - \\ c_{3x}|e_{i,x}|^{\alpha_x}\mathrm{sgn}(e_{i,x}) \Big) \\ \frac{1}{c_{1y}(\sum_{j=1}^{N} a_{ij} + b_i)} \Big(c_{1y}(\sum_{j=1}^{N} a_{ij}\ddot{y}_j + b_i\ddot{y}_0) + \\ c_{1y}(\sum_{j=1}^{N} a_{ij} + b_i)\bar{k}_{i,y}\dot{y}_i - c_{2y}\dot{e}_{i,y} - \\ c_{3y}|e_{i,y}|^{\alpha_y}\mathrm{sgn}(e_{i,y}) \Big) \\ \frac{1}{c_{1z}(\sum_{j=1}^{N} a_{ij} + b_i)} \Big(c_{1z}(\sum_{j=1}^{N} a_{ij}\ddot{z}_j + b_i\ddot{z}_0) + \\ c_{1z}(\sum_{j=1}^{N} a_{ij} + b_i)\bar{k}_{i,z}\dot{z}_i - c_{2z}\dot{e}_{i,z} - \\ c_{3z}|e_{i,z}|^{\alpha_z}\mathrm{sgn}(e_{i,z}) \Big) \end{bmatrix} \tag{15}$$

To achieve fast convergence of the i-th quadrotor's states to the sliding surfaces $s_{i,x}, s_{i,y}$, and $s_{i,z}$, the following reaching

control law is designed:

$$\begin{bmatrix} u^{\mathrm{r}}_{i,x} \\ u^{\mathrm{r}}_{i,y} \\ u^{\mathrm{r}}_{i,z} \end{bmatrix} = \begin{bmatrix} \frac{1}{c_{1x}(\sum_{j=1}^{N} a_{ij}+b_i)} \left(-\widehat{k}^x_1 s_{i,x} - \widehat{k}^x_2 |s_{i,x}|^{\lambda_x} \mathrm{sign}(s_{i,x})\right) \\ \frac{1}{c_{1y}(\sum_{j=1}^{N} a_{ij}+b_i)} \left(-\widehat{k}^y_1 s_{i,y} - \widehat{k}^y_2 |s_{i,y}|^{\lambda_y} \mathrm{sign}(s_{i,y})\right) \\ \frac{1}{c_{1z}(\sum_{j=1}^{N} a_{ij}+b_i)} \left(-\widehat{k}^z_1 s_{i,z} - \widehat{k}^z_2 |s_{i,z}|^{\lambda_z} \mathrm{sign}(s_{i,z})\right) \end{bmatrix} \tag{16}$$

where the exponents $\lambda_x, \lambda_y, \lambda_z$ satisfy $0 < \lambda_\kappa < 1$ for $\kappa = (x, y, z)$, and the coefficients $\widehat{k}^x_1, \widehat{k}^x_2, \widehat{k}^y_1, \widehat{k}^y_2, \widehat{k}^z_1, \widehat{k}^z_2$ are the estimates of $k^x_1, k^x_2, k^y_1, k^y_2, k^z_1, k^z_2$ and are updated using the following adaptive laws:

$$\begin{bmatrix} \dot{\widehat{k}}^x_1 \\ \dot{\widehat{k}}^y_1 \\ \dot{\widehat{k}}^z_1 \end{bmatrix} = \begin{bmatrix} \rho^x_1 |s_{i,x}|^2 \\ \rho^y_1 |s_{i,y}|^2 \\ \rho^z_1 |s_{i,z}|^2 \end{bmatrix}, \begin{bmatrix} \dot{\widehat{k}}^x_2 \\ \dot{\widehat{k}}^y_2 \\ \dot{\widehat{k}}^z_2 \end{bmatrix} = \begin{bmatrix} \rho^x_2 |s_{i,x}|^{\lambda_x+1} \\ \rho^y_2 |s_{i,y}|^{\lambda_y+1} \\ \rho^z_2 |s_{i,z}|^{\lambda_z+1} \end{bmatrix}. \tag{17}$$

where $\rho^\kappa_1, \rho^\kappa_2$ for $\kappa = (x, y, z)$ are positive constants.

Remark 1: The adaptive laws designed in equation (17) ensure a robust and reliable control system for the quadrotors, particularly in agricultural environments characterized by external disturbances and obstacles. These laws allow the system to dynamically adjust control actions, ensuring efficient flight formation and safe collision avoidance while maintaining formation stability throughout the mission.

Thus, the virtual control inputs are defined as:

$$\begin{bmatrix} f_{i,x} \\ f_{i,y} \\ f_{i,z} \end{bmatrix} = \begin{bmatrix} u^{\mathrm{eq}}_{i,x} + u^{\mathrm{r}}_{i,x} \\ u^{\mathrm{eq}}_{i,y} + u^{\mathrm{r}}_{i,y} \\ u^{\mathrm{eq}}_{i,z} + u^{\mathrm{r}}_{i,z} \end{bmatrix} \tag{18}$$

By substituting the equivalent control laws (15) and the reaching control laws (16) into (18), the virtual control inputs for the position dynamics of the i-th quadrotor are obtained:

$$\begin{bmatrix} f_{i,x} \\ f_{i,y} \\ f_{i,z} \end{bmatrix} = \begin{bmatrix} \frac{1}{c_{1x}(\sum_{j=1}^{N} a_{ij}+b_i)} \Big(c_{1x}(\sum_{j=1}^{N} a_{ij}\ddot{x}_j + b_i\ddot{x}_0) + \\ c_{1x}(\sum_{j=1}^{N} a_{ij} + b_i)\bar{k}_{i,x}\dot{x}_i - c_{2x}\dot{e}_{i,x} - \\ c_{3x}|e_{i,x}|^{\alpha_x}\mathrm{sgn}(e_{i,x}) - \\ \widehat{k}^x_1 s_{i,x} - \widehat{k}^x_2 |s_{i,x}|^{\lambda_x}\mathrm{sign}(s_{i,x}) \Big) \\ \frac{1}{c_{1y}(\sum_{j=1}^{N} a_{ij}+b_i)} \Big(c_{1y}(\sum_{j=1}^{N} a_{ij}\ddot{y}_j + b_i\ddot{y}_0) + \\ c_{1y}(\sum_{j=1}^{N} a_{ij} + b_i)\bar{k}_{i,y}\dot{y}_i - c_{2y}\dot{e}_{i,y} - \\ c_{3y}|e_{i,y}|^{\alpha_y}\mathrm{sgn}(e_{i,y}) - \\ \widehat{k}^y_1 s_{i,y} - \widehat{k}^y_2 |s_{i,y}|^{\lambda_y}\mathrm{sign}(s_{i,y}) \Big) \\ \frac{1}{c_{1z}(\sum_{j=1}^{N} a_{ij}+b_i)} \Big(c_{1z}(\sum_{j=1}^{N} a_{ij}\ddot{z}_j + b_i\ddot{z}_0) + \\ c_{1z}(\sum_{j=1}^{N} a_{ij} + b_i)\bar{k}_{i,z}\dot{z}_i - c_{2z}\dot{e}_{i,z} - \\ c_{3z}|e_{i,z}|^{\alpha_z}\mathrm{sgn}(e_{i,z}) - \\ \widehat{k}^z_1 s_{i,z} - \widehat{k}^z_2 |s_{i,z}|^{\lambda_z}\mathrm{sign}(s_{i,z}) \Big) \end{bmatrix} \tag{19}$$

Theorem 1: Considering the translational dynamic model given in (1), the sliding surfaces defined in (13), and the control law designed in (19), the states of the translational dynamic system will converge to the sliding surfaces (13) in finite time. Consequently, the tracking errors defined in (11) will also converge to the origin in finite time.

Proof 1: In order to prove Theorem 1, we define the following Lyapunov function:

$$V_x = \frac{1}{2}(s_{i,x})^2. \tag{20}$$

Deriving the time V_x and replacing the expression (14) we obtain the following:

$$\begin{aligned} \dot{V}_x =& s_{i,x}\big[\dot{s}_{i,x}\big] \\ =& s_{i,x}\big[c_{1x}(\sum_{j=1}^{N} a_{ij}(\ddot{x}_i - \ddot{x}_j) + b_i(\ddot{x}_i - \ddot{x}_0)) + \\ & c_{2x}\dot{e}_{i,x} + c_{3x}|e_{i,x}|^{\alpha_x}\mathrm{sgn}(e_{i,x})\big] \\ =& s_{i,x}\big[-k^x_1 s_{i,x} - k^x_2 |s_{i,x}|^{\lambda_x}\mathrm{sign}(s_{i,x})\big] \\ =& -k^x_1 (s_{i,x})^2 - k^x_2 (s_{i,x})^{\lambda_x+1} \end{aligned} \tag{21}$$

By performing some mathematical operations, we obtain:

$$\dot{V}_x = -2k^x_1\big[V_x\big] - 2^{\frac{\lambda_x+1}{2}} k^x_2 \big[V_x\big]^{\frac{\lambda_x+1}{2}} \tag{22}$$

According to Lemma 1, the states of the translational dynamic system "x" reach the sliding surface $s_{i,x}$ in a finite time given by:

$$T^f_x = \frac{2}{k^x_1(1-\lambda_x)} \ln\Big(\frac{k^x_2 + k^x_1 (V_x(0))^{\frac{1-\lambda_x}{2}}}{k^x_2}\Big). \tag{23}$$

Remark 2: By applying the same procedure as in Proof 1, it follows that the states "y" and "z" of the translational dynamic system converge to the sliding surfaces $s_{i,y}$ and $s_{i,z}$ in finite times T^f_y and T^f_z, respectively.

2) Attitude Control: In this subsection, we design the control inputs $(u_{i,\phi}, u_{i,\theta}, u_{i,\psi})$ for the rotational dynamics control of the i-th quadrotor. To achieve this, we define the attitude tracking errors and their derivatives as follows:

$$\begin{aligned} \begin{bmatrix} e_{i,\phi} \\ e_{i,\theta} \\ e_{i,\psi} \end{bmatrix} &= \begin{bmatrix} \phi_i - \phi^d_i \\ \theta_i - \theta^d_i \\ \psi_i - \psi^d_i \end{bmatrix} \\ \begin{bmatrix} \dot{e}_{i,\phi} \\ \dot{e}_{i,\theta} \\ \dot{e}_{i,\psi} \end{bmatrix} &= \begin{bmatrix} \dot{\phi}_i - \dot{\phi}^d_i \\ \dot{\theta}_i - \dot{\theta}^d_i \\ \dot{\psi}_i - \dot{\psi}^d_i \end{bmatrix} \end{aligned} \tag{24}$$

To ensure that the attitude tracking errors converge to zero, we propose the following integral sliding surface:

$$\begin{bmatrix} s_{i,\phi} \\ s_{i,\theta} \\ s_{i,\psi} \end{bmatrix} = \begin{bmatrix} c_{1\phi}\dot{e}_{i,\phi} + c_{2\phi}e_{i,\phi} + c_{3\phi}\int_0^t [|e_{i,\phi}|^{\alpha_\phi}\mathrm{sgn}(e_{i,\phi})]dt \\ c_{1\theta}\dot{e}_{i,\theta} + c_{2\theta}e_{i,\theta} + c_{3\theta}\int_0^t [|e_{i,\theta}|^{\alpha_\theta}\mathrm{sgn}(e_{i,\theta})]dt \\ c_{1\psi}\dot{e}_{i,\psi} + c_{2\psi}e_{i,\psi} + c_{3\psi}\int_0^t [|e_{i,\psi}|^{\alpha_\psi}\mathrm{sgn}(e_{i,\psi})]dt \end{bmatrix} \tag{25}$$

where $c_{1\kappa}, c_{2\kappa}, c_{3\kappa}$ con $\kappa = (\phi, \theta, \psi)$ are positive constants representing the controller parameters. The exponents $\alpha_\phi, \alpha_\theta, \alpha_\psi$ satisfy the inequality $0 < \alpha_\kappa < 1$ con $\kappa = (\phi, \theta, \psi)$. Taking the time derivative of the sliding surfaces gives:

$$\begin{bmatrix} \dot{s}_{i,\phi} \\ \dot{s}_{i,\theta} \\ \dot{s}_{i,\psi} \end{bmatrix} = \begin{bmatrix} c_{1\phi}\ddot{e}_{i,\phi} + c_{2\phi}\dot{e}_{i,\phi} + c_{3\phi}|e_{i,\phi}|^{\alpha_\phi}\mathrm{sgn}(e_{i,\phi}) \\ c_{1\theta}\ddot{e}_{i,\theta} + c_{2\theta}\dot{e}_{i,\theta} + c_{3\theta}|e_{i,\theta}|^{\alpha_\theta}\mathrm{sgn}(e_{i,\theta}) \\ c_{1\psi}\ddot{e}_{i,\psi} + c_{2\psi}\dot{e}_{i,\psi} + c_{3\psi}|e_{i,\psi}|^{\alpha_\psi}\mathrm{sgn}(e_{i,\psi}) \end{bmatrix} \tag{26}$$

By enforcing the sliding mode condition $\dot{s}_{i,\phi} = \dot{s}_{i,\theta} = \dot{s}_{i,\psi} = 0$, the equivalent control law is designed as follows:

$$\begin{bmatrix} u_{i,\phi}^{\text{eq}} \\ u_{i,\theta}^{\text{eq}} \\ u_{i,\psi}^{\text{eq}} \end{bmatrix} = \begin{bmatrix} \frac{J_{i,x}}{c_{1\phi}}\Big(-c_{1\phi}J_{i,x}^{-1}\big[(J_{i,y}-J_{i,z})\dot{\theta}_i\dot{\psi}_i- \\ J_{i,r}\dot{\theta}_i\overline{\omega}_i-\bar{k}_{i,\phi}\dot{\phi}_i^2\big]-c_{2\phi}\dot{e}_{i,\phi}- \\ c_{3\phi}|e_{i,\phi}|^{\alpha_\phi}\text{sgn}(e_{i,\phi})+c_{1\phi}\ddot{\phi}_i^d\Big) \\ \frac{J_{i,y}}{c_{1\theta}}\Big(-c_{1\theta}J_{i,x}^{-1}\big[(J_{i,y}-J_{i,z})\dot{\theta}_i\dot{\psi}_i- \\ J_{i,r}\dot{\theta}_i\overline{\omega}_i-\bar{k}_{i,\phi}\dot{\phi}_i^2\big]-c_{2\theta}\dot{e}_{i,\theta}- \\ c_{3\theta}|e_{i,\theta}|^{\alpha_\theta}\text{sgn}(e_{i,\theta})+c_{1\theta}\ddot{\theta}_i^d\Big) \\ \frac{J_{i,z}}{c_{1\psi}}\Big(-c_{1\psi}J_{i,z}^{-1}\big[(J_{i,x}-J_{i,y})\dot{\phi}_i\dot{\theta}_i- \\ \bar{k}_{i,\psi}\dot{\psi}_i^2\big]-c_{2\psi}\dot{e}_{i,\psi}- \\ c_{3\psi}|e_{i,\psi}|^{\alpha_\psi}\text{sgn}(e_{i,\psi})+c_{1\psi}\ddot{\psi}_i^d\Big) \end{bmatrix} \tag{27}$$

To achieve fast convergence of the i-th quadrotor's states to the sliding surfaces $s_{i,\phi}$, $s_{i,\theta}$, and $s_{i,\psi}$, the following reaching control law is designed:

$$\begin{bmatrix} u_{i,\phi}^{\text{r}} \\ u_{i,\theta}^{\text{r}} \\ u_{i,\psi}^{\text{r}} \end{bmatrix} = \begin{bmatrix} \frac{J_{i,x}}{c_{1\phi}}\big(-k_1^\phi s_{i,\phi}-k_2^\phi|s_{i,\phi}|^{\lambda_\phi}\text{sign}(s_{i,\phi})\big) \\ \frac{J_{i,y}}{c_{1\theta}}\big(-k_1^\theta s_{i,\theta}-k_2^\theta|s_{i,\theta}|^{\lambda_\theta}\text{sign}(s_{i,\theta})\big) \\ \frac{J_{i,z}}{c_{1\psi}}\big(-k_1^\psi s_{i,\psi}-k_2^\psi|s_{i,\psi}|^{\lambda_\psi}\text{sign}(s_{i,\psi})\big) \end{bmatrix} \tag{28}$$

where the exponents $\lambda_\phi, \lambda_\theta, \lambda_\psi$ satisfy $0 < \lambda_\kappa < 1$ for $\kappa = (\phi, \theta, \psi)$, and the coefficients $\widehat{k}_1^\phi, \widehat{k}_2^\phi, \widehat{k}_1^\theta, \widehat{k}_2^\theta, \widehat{k}_1^\psi, \widehat{k}_2^\psi$ are the estimates of $k_1^\phi, k_2^\phi, k_1^\theta, k_2^\theta, k_1^\psi, k_2^\psi$ and are updated using the following adaptive laws:

$$\begin{bmatrix} \dot{\widehat{k}}_1^\phi \\ \dot{\widehat{k}}_1^\theta \\ \dot{\widehat{k}}_1^\psi \end{bmatrix} = \begin{bmatrix} \rho_1^\phi|s_{i,\phi}|^2 \\ \rho_1^\theta|s_{i,\theta}|^2 \\ \rho_1^\psi|s_{i,\psi}|^2 \end{bmatrix}, \begin{bmatrix} \dot{\widehat{k}}_2^\phi \\ \dot{\widehat{k}}_2^\theta \\ \dot{\widehat{k}}_2^\psi \end{bmatrix} = \begin{bmatrix} \rho_2^\phi|s_{i,\phi}|^{\lambda_\phi+1} \\ \rho_2^\theta|s_{i,y}|^{\lambda_\theta+1} \\ \rho_2^\psi|s_{i,\psi}|^{\lambda_\psi+1} \end{bmatrix}. \tag{29}$$

where $\rho_1^\kappa, \rho_2^\kappa$ for $\kappa = (\phi, \theta, \psi)$ are positive constants.

Thus, the attitude control inputs are defined as follows:

$$\begin{bmatrix} u_{i,\phi} \\ u_{i,\theta} \\ u_{i,\psi} \end{bmatrix} = \begin{bmatrix} u_{i,\phi}^{\text{eq}} + u_{i,\phi}^{\text{r}} \\ u_{i,\theta}^{\text{eq}} + u_{i,\theta}^{\text{r}} \\ u_{i,\psi}^{\text{eq}} + u_{i,\psi}^{\text{r}} \end{bmatrix} \tag{30}$$

By substituting the equivalent control laws (27) and the reaching control laws (28) into (30), the control inputs for the rotational dynamics of the i-th quadrotor are obtained:

$$\begin{bmatrix} u_{i,\phi} \\ u_{i,\theta} \\ u_{i,\psi} \end{bmatrix} = \begin{bmatrix} \frac{J_{i,x}}{c_{1\phi}}\Big(-c_{1\phi}J_{i,x}^{-1}\big[(J_{i,y}-J_{i,z})\dot{\theta}_i\dot{\psi}_i- \\ J_{i,r}\dot{\theta}_i\overline{\omega}_i-\bar{k}_{i,\phi}\dot{\phi}_i^2\big]-c_{2\phi}\dot{e}_{i,\phi}- \\ c_{3\phi}|e_{i,\phi}|^{\alpha_\phi}\text{sgn}(e_{i,\phi})+c_{1\phi}\ddot{\phi}_i^d- \\ \widehat{k}_1^\phi s_{i,\phi}-\widehat{k}_2^\phi|s_{i,\phi}|^{\lambda_\phi}\text{sign}(s_{i,\phi})\Big) \\ \frac{J_{i,y}}{c_{1\theta}}\Big(-c_{1\theta}J_{i,x}^{-1}\big[(J_{i,y}-J_{i,z})\dot{\theta}_i\dot{\psi}_i- \\ J_{i,r}\dot{\theta}_i\overline{\omega}_i-\bar{k}_{i,\phi}\dot{\phi}_i^2\big]-c_{2\theta}\dot{e}_{i,\theta}- \\ c_{3\theta}|e_{i,\theta}|^{\alpha_\theta}\text{sgn}(e_{i,\theta})+c_{1\theta}\ddot{\theta}_i^d- \\ \widehat{k}_1^\theta s_{i,\theta}-\widehat{k}_2^\theta|s_{i,\theta}|^{\lambda_\theta}\text{sign}(s_{i,\theta})\Big) \\ \frac{J_{i,z}}{c_{1\psi}}\Big(-c_{1\psi}J_{i,z}^{-1}\big[(J_{i,x}-J_{i,y})\dot{\phi}_i\dot{\theta}_i- \\ \bar{k}_{i,\psi}\dot{\psi}_i^2\big]-c_{2\psi}\dot{e}_{i,\psi}- \\ c_{3\psi}|e_{i,\psi}|^{\alpha_\psi}\text{sgn}(e_{i,\psi})+c_{1\psi}\ddot{\psi}_i^d- \\ \widehat{k}_1^\psi s_{i,\psi}-\widehat{k}_2^\psi|s_{i,\psi}|^{\lambda_\psi}\text{sign}(s_{i,\psi})\Big) \end{bmatrix} \tag{31}$$

Remark 3: By following the same procedure as in Theorem 1, it is concluded that the states of the rotational dynamic system converge to their sliding surfaces in finite time. Consequently, the tracking errors defined in (24) also converge to the origin in finite time.

C. Stability Analysis

Theorem 2: Considering the system (1), along with the sliding surfaces (13) and (25), the control laws designed in (19) and (31), together with the adaptive laws in (17) and (29), will drive the tracking errors to the origin in finite time. Consequently, the states of the system (1) will reach their desired values in finite time.

Proof 2: We define the following Lyapunov candidate function as follows:

$$V = \frac{1}{2}(s_{i,x})^2 + \frac{1}{2\rho_1}(\tilde{k}_1^x)^2 + \frac{1}{2\rho_2}(\tilde{k}_2^x)^2, \tag{32}$$

where $\tilde{k}_1^x$ and $\tilde{k}_2^x$ are the adaptive estimation errors. Then $\tilde{k}_1^x = \widehat{k}_1^x - k_1^x$, $\tilde{k}_2^x = \widehat{k}_2^x - k_2^x$.

Deriving in time (32) and performing the corresponding mathematical operations, we obtain the following expression:

$$\begin{aligned} \dot{V} =& s_{i,x}(\dot{s}_{i,x}) + \frac{\tilde{k}_1^x}{\rho_1^x}(\dot{\tilde{k}}_1^x) + \frac{\tilde{k}_2^x}{\rho_2^x}(\dot{\tilde{k}}_2^x) \\ \dot{V} =& s_{i,x}\big[c_{1x}(\sum_{j=1}^{N} a_{ij}(\ddot{x}_i - \ddot{x}_j) + b_i(\ddot{x}_i - \ddot{x}_0)) + \\ & c_{2x}\dot{e}_{i,x} + c_{3x}|e_{i,x}|^{\alpha_x}\text{sgn}(e_{i,x})\big] + \frac{\tilde{k}_1^x}{\rho_1^x}(\dot{\tilde{k}}_1^x) + \frac{\tilde{k}_2^x}{\rho_2^x}(\dot{\tilde{k}}_2^x) \\ =& s_{i,x}\big[c_{1x}\big(\sum_{j=1}^{N} a_{ij} + b_i\big)(f_{i,x} - \bar{k}_{i,x}\dot{x}_i) - c_{1x}\big(\sum_{j=1}^{N} a_{ij} + b_i\ddot{x}_0\big) + \\ & c_{2x}\dot{e}_{i,x} + c_{3x}|e_{i,x}|^{\alpha_x}\text{sgn}(e_{i,x})\big] + \frac{\tilde{k}_1^x}{\rho_1^x}(\dot{\tilde{k}}_1^x) + \frac{\tilde{k}_2^x}{\rho_2^x}(\dot{\tilde{k}}_2^x) \\ =& s_{i,x}\big[u_{i,x}^{\text{r}}\big] + \frac{\tilde{k}_1^x}{\rho_1^x}(\dot{\tilde{k}}_1^x) + \frac{\tilde{k}_2^x}{\rho_2^x}(\dot{\tilde{k}}_2^x) \end{aligned} \tag{33}$$

Substituting the reaching control law given in (16) and the adaptive laws given in (17) into expression (33), we obtain:

$$\begin{aligned}\dot{V} =& s_{i,x}\big(-\widehat{k}_1^x s_{i,x} - \widehat{k}_2^x |s_{i,x}|^{\lambda_x}\text{sign}(s_{i,x})\big)+\\ & \frac{\tilde{k}_1^x}{\rho_1^x}(\dot{\tilde{k}}_1^x) + \frac{\tilde{k}_2^x}{\rho_2^x}(\dot{\tilde{k}}_2^x)\\ =&\big(-\widehat{k}_1^x|s_{i,x}|^2 - \widehat{k}_2^x|s_{i,x}|^{\lambda_x+1}\big) + \frac{\tilde{k}_1^x}{\rho_1^x}(\dot{\widehat{k}}_1^x)+\\ & \frac{\tilde{k}_2^x}{\rho_2^x}(\dot{\widehat{k}}_2^x) + \big(k_1^x|s_{i,x}|^2 - k_1^x|s_{i,x}|^2+\\ & k_2^x|s_{i,x}|^{\lambda_x+1} - k_2^x|s_{i,x}|^{\lambda_x+1}\big)\\ =& -\widehat{k}_1^x|s_{i,x}|^2 - \widehat{k}_2^x|s_{i,x}|^{\lambda_x+1} + \frac{\tilde{k}_1^x}{\rho_1^x}(\rho_1^x|s_{i,x}|^2)+\\ & \frac{\tilde{k}_2^x}{\rho_2^x}(\rho_2^x|s_{i,x}|^{\lambda_x+1}) + k_1^x|s_{i,x}|^2 - k_1^x|s_{i,x}|^2+\\ & k_2^x|s_{i,x}|^{\lambda_x+1} - k_2^x|s_{i,x}|^{\lambda_x+1}\\ =& -(\tilde{k}_1^x)|s_{i,x}|^2 - (\tilde{k}_2^x)|s_{i,x}|^{\lambda_x+1} + \frac{\tilde{k}_1^x}{\rho_1^x}(\rho_1^x|s_{i,x}|^2)+\\ & \frac{\tilde{k}_2^x}{\rho_2^x}(\rho_2^x|s_{i,x}|^{\lambda_x+1}) - k_1^x|s_{i,x}|^2 - k_2^x|s_{i,x}|^{\lambda_x+1}\\ =& -\tilde{k}_1^x(|s_{i,x}|^2 - |s_{i,x}|^2) - \tilde{k}_2^x(|s_{i,x}|^{\lambda_x+1} - |s_{i,x}|^{\lambda_x+1})-\\ & k_1^x|s_{i,x}|^2 - k_2^x|s_{i,x}|^{\lambda_x+1}\\ V \leq& -k_1^x|s_{i,x}|^2 - k_2^x|s_{i,x}|^{\lambda_x+1}\end{aligned} \tag{34}$$

From expression (34), we can conclude that $s_{i,x}$ converges to zero in a finite time. Moreover, the convergence of the adaptive parameters $\tilde{k}_1^x$ and $\tilde{k}_2^x$ are also ensured.

V. Results and Discussions

This section evaluates the effectiveness of the proposed control framework through numerical simulations in the MATLAB/Simulink environment using the block diagram shown in Fig. 2.

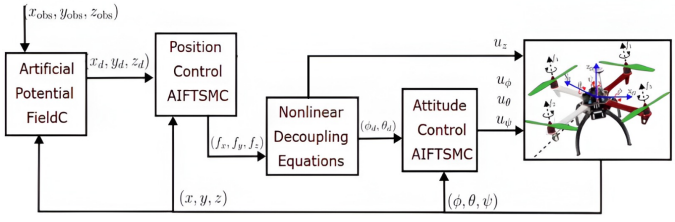

Fig. 2. Proposed Control Block Diagram.

The proposed control system for cooperative multi-quadrotor formation in agricultural environments with obstacles and external disturbances is based on a robust control approach implemented in MATLAB/Simulink. Initially, the APF module receives the coordinates of the obstacles $(x_{\text{obs}}, y_{\text{obs}}, z_{\text{obs}})$ and generates a reference trajectory for the i_{th} quadcopter (x_d, y_d, z_d) to avoid collisions. Then, the AIFTSMC position controller computes the control forces (f_x, f_y, f_z) by comparing the reference with the current position (x, y, z). These forces are transformed into the desired inclination angles (ϕ_d, θ_d) and (u_z) through nonlinear decoupling equations, facilitating attitude and position control, respectively. Subsequently, the AIFTSMC attitude controller adjusts the control signals $(u_\phi, u_\theta, u_\psi)$ to stabilize the quadrotor's orientation. Finally, the quadrotor's dynamic model executes these control signals, while state feedback continuously updates the control system, ensuring stable and precise flight. The block diagram represented in the Fig. 2, is the same for the three quadcopters under guide of the Artificial Potential Field (APF) module.

TABLE I
Control System Parameters

Parameter	Value	Parameter	Value
c_{1x}, c_{1y}, c_{1z}	1	$\rho_1^x, \rho_1^y, \rho_1^z$	1.2
c_{2x}, c_{2y}, c_{2z}	2.031	$\rho_2^x, \rho_2^y, \rho_2^z$	3
c_{3x}, c_{3y}, c_{3z}	0.051	$\lambda_x, \lambda_y, \lambda_z$	1.2
$c_{1\phi}, c_{1\theta}, c_{1\psi}$	1.5	$\lambda_\phi, \lambda_\theta, \lambda_\psi$	1.2
$c_{2\phi}, c_{2\theta}, c_{2\psi}$	12	$\rho_1^\phi, \rho_1^\theta, \rho_1^\psi$	2
$c_{3\phi}, c_{3\theta}, c_{3\psi}$	0.2	$\rho_2^\phi, \rho_2^\theta, \rho_2^\psi$	4
$\alpha_x, \alpha_y, \alpha_z$	0.25	k_a	3
$\alpha_\phi, \alpha_\theta, \alpha_\psi$	0.2	k_r	0.5

A typical agricultural scenario [26] is implemented, simulating a 160-square-meter crop area where the quadrotors must fully cover the zone, encountering both obstacles and external disturbances caused by wind. The flight formation consists of three quadrotors (QUAVs), with the first QUAV acting as the group leader while the remaining two follow. Communication between the aerial vehicles is managed using graph theory, represented by a directed graph. The formation pattern is set in a straight line with a 1-meter distance between agents, as shown in Fig. 3.

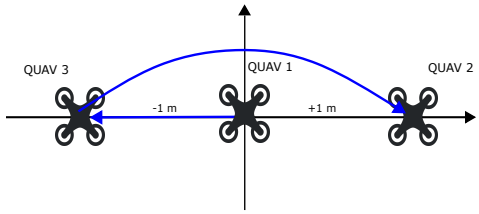

Fig. 3. Communication topology and formation pattern.

The adjacency matrix, the degree matrix, the Laplacian matrix, and the leader matrix are defined as:

$$A = \begin{bmatrix}0 & 0\\ 1 & 0\end{bmatrix}, D = \begin{bmatrix}0 & 0\\ 0 & 1\end{bmatrix}, L = \begin{bmatrix}0 & 0\\ -1 & 1\end{bmatrix} B = \begin{bmatrix}1 & 0\\ 0 & 0\end{bmatrix} \tag{35}$$

The physical parameters of the aerial vehicles are: $m_i = 1.6\text{kg}$, $J_i = \text{diag}(0.0232, 0.0249, 0.0342)\text{kgm}^2$, $l = 0.2\text{m}$ and $g = 9.8\text{m/s}^2$. The parameters of the proposed control framework are presented in Table 1.

The initial positions of the three quadrotors are set as: $\xi_1(0) = [0.5, 0.5, 0.01]^T, \text{m}$, $\xi_2(0) = [-1, -2, 0.01]^T, \text{m}$ y $\xi_3(0) = [-1, 2, 0.01]^T, \text{m}$. Throughout the trajectory, the quadrotors must avoid three strategically placed obstacles

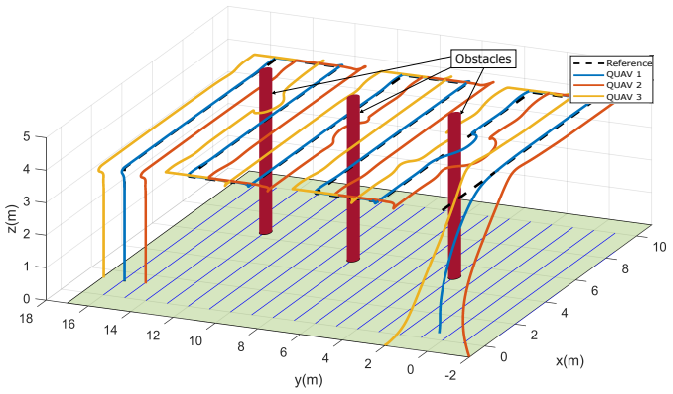

Fig. 4. 3D flight formation of the agricultural scenery.

in the environment. Additionally, they are subjected to external disturbances caused by wind, modeled as: $d_{i,\xi}^{ext} = [0.5\cos(0.5t) + 0.5\sin(0.5t), 0.6\sin(0.2t) + 0.4\cos(0.4t), 0.5\cos(0.5t)]^T$, (N.) and $d_{i,\eta}^{ext} = [0.1\cos(t), 0.1\sin(t), 0.5\cos(0.5t)]^T$, (N.m.).

Fig. 4 presents a 3D view of the simulation of the formation flight of three quadrotors (QUAVs) in an agricultural environment with the presence of three obstacles and external disturbances. The simulation demonstrates the effectiveness of the proposed control framework, which integrates a guidance system based on the Artificial Potential Field (APF) algorithm (10) and an advanced formation controller, AIFTSMC (19), (31). As seen in the figure, the three quadrotors successfully follow the desired formation trajectory, effectively avoiding obstacles, fully covering the assigned agricultural area, and maintaining stable formation throughout the entire flight mission.

The temporal evolution of the quadrotors' positions and linear velocities is shown in Figs. 5 and 6. In Fig. 5, it can be observed that despite external disturbances, the proposed system ensures robust formation trajectory tracking. The three obstacles along the route are effectively avoided: the group leader faces the first obstacle, while followers 2 and 3 avoid the second and third obstacles, respectively. The quadrotors successfully avoid the obstacles without significantly deviating from the formation. This behavior highlights the capability of the guidance system to autonomously manage obstacle avoidance and quickly restore the desired trajectory after each evasive maneuver.

Fig. 7 shows the temporal evolution of the formation tracking errors, with fast convergence to zero. The system manages to keep the errors within a small neighborhood around zero, even in the presence of external disturbances. Fig. 8 illustrates the relative distances between the quadrotors. The desired formation pattern, with 2-meter distances between the followers and 1 meter relative to the leader, is consistently maintained throughout the flight mission, reflecting high precision in the formation dynamics.

Furthermore, the temporal evolution of the attitude of the quadrotors, represented by Euler angles, is shown in Fig. 9. The angles stabilize at the desired references, underscoring the controller's ability to maintain proper orientation in

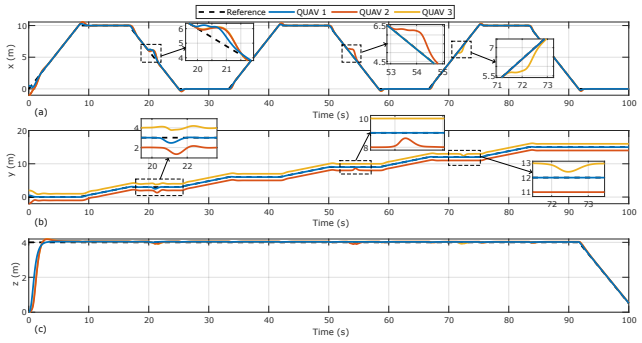

Fig. 5. Evolution in time of quadrotor position: a) In X, b) In Y, and c) In Z.

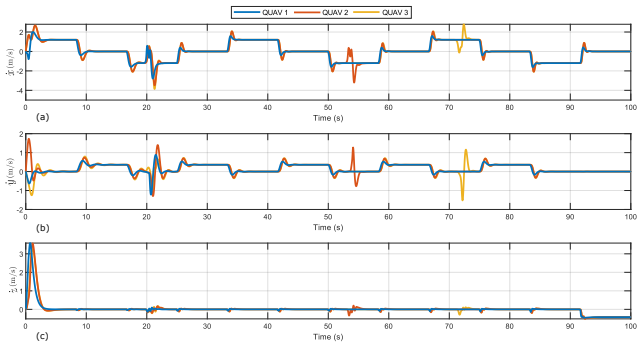

Fig. 6. Evolution in time of the linear velocity: a) In X, b) In Y, and c) In Z.

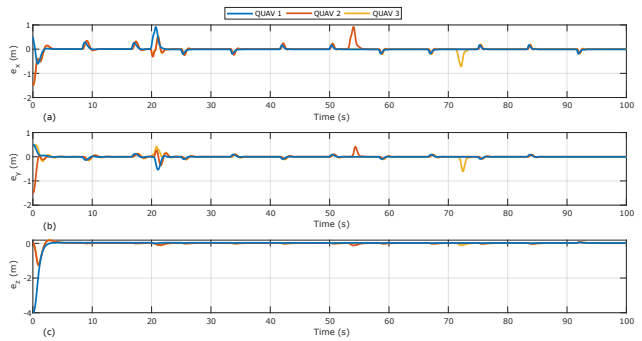

Fig. 7. Evolution in time of formation errors: a) In X, b) In Y, and c) In Z.

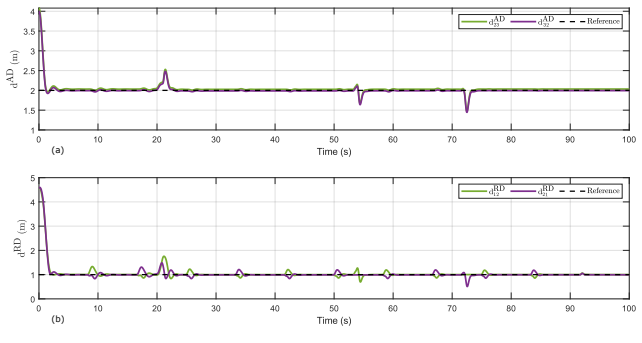

Fig. 8. Distance between quadrotors: a) Between followers, and b) Between leader and follower.

the presence of disturbances. Fig. 10 displays the applied control signals, verifying their smoothness and effectiveness

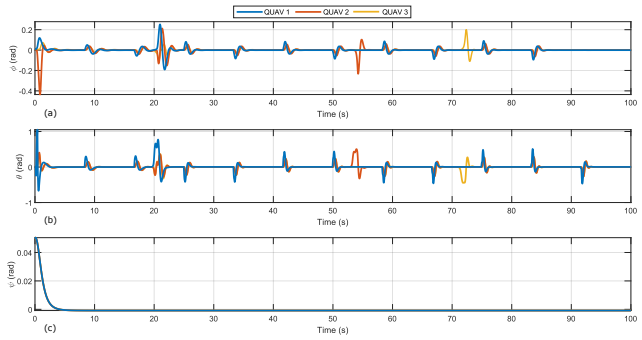

Fig. 9. Evolution in time of the attitude of quadrotor: a) In ϕ, b) In θ, and c) In ψ.

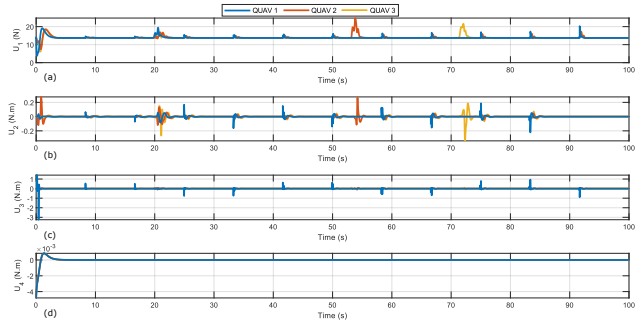

Fig. 10. Evolution in time of the control inputs: a) In Z, b) In roll, c) In pitch and d) In yaw

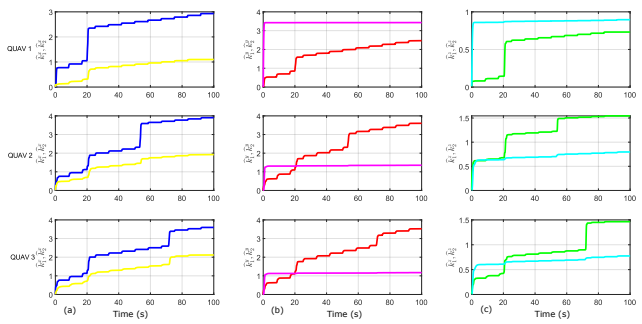

Fig. 11. Evolution in time of adaptive gains of quadrotor 1, 2 and 3: a) In X, b) In Y, and c) In Z.

throughout the mission. Finally, Fig. 11 illustrates the adaptive gains of the AIFTSMC system, which dynamically adjust the control parameters in response to environmental variations, confirming the adaptability and robustness of the proposed control framework.

VI. Conclusions

In this paper, a distributed autonomous control framework for multi-quadrotor formation flight in agricultural scenarios has been proposed. This framework integrates both a guidance system and a control system for each quadrotor. The Artificial Potential Field (APF) algorithm is implemented in the guidance system, while a distributed consensus protocol based on the Adaptive Integral Fast Terminal Sliding Mode Control (AIFTSMC) strategy is designed for formation control.

The results obtained through numerical simulations confirm the effectiveness of the proposed framework in agricultural environments characterized by the presence of obstacles and external disturbances. The approach achieved complete coverage of the agricultural area while maintaining the desired formation pattern between the quadrotors throughout the flight mission. Furthermore, it demonstrated remarkable capability in obstacle avoidance and quickly restoring the desired trajectory, maintaining the stability of the formation pattern during the entire mission. The adaptive laws allow for dynamic adjustment of control actions, providing robust and reliable system control in the presence of external disturbances.

In future work, we propose experimental validation using the proposed algorithm and control, comparing it with other control laws in complex agricultural scenarios. The algorithms and controls can be implemented in a distributed autonomous control framework such us PX4-Autopilot on DJI-F450 quadrotors.

Acknowledgments

The authors thank the Instituto de Investigación Astronómico y Aeroespacial Pedro Paulet, IAAPP-UNSA.

References

[1] Santos, S., Givigi, S., Nascimento, C., Fernandes, J., Buonocore, L. and Almeida Neto, A. “Iterative decentralized planning for collective construction tasks with quadrotors,” *J. Intell. Robot. Syst.*, vol. 90, pp. 217-234, Oct. 2017, doi: 10.1007/s10846-017-0659-6.

[2] Khalil, H., Rahman, S., Ullah, I., Khan, I., Alghadhban, A., Al-Adhaileh, M., Ali, G. and ElAffendi, M. “A uav-swarm-communication model using a machine-learning approach for search-and-rescue applications,” *Drones*, vol. 6, pp. 12, Nov. 2022, doi: 10.3390/drones6120372.

[3] Chin, R., Catal, C. and Kassahun, A. “Plant disease detection using drones in precision agriculture,” *Precision Agric.*, vol. 24, pp. 1663-1682, Mar. 2023, doi: 10.1007/s11119-023-10014-y.

[4] Mogili, U. and Deepak, B. “Review on application of drone systems in precision agriculture,” *Procedia Comput. Sci.*, vol. 133, pp. 502-509, 2018, doi: 10.1016/j.procs.2018.07.063.

[5] Rahman, M., Fan, S., Zhang, Y. and Chen, L. “A comparative study on application of unmanned aerial vehicle systems in agriculture,” *Agriculture*, vol. 11, pp. 22, Jan. 2021, doi: 10.3390/agriculture11010022.

[6] Kim, J., Kim, S., Ju, C. and Son, H. “Unmanned aerial vehicles in agriculture: A review of perspective of platform, control, and applications,” *IEEE Access*, vol. 7, pp. 105100-105115, Jul. 2019, doi: 10.1109/ACCESS.2019.2932119.

[7] Huang, J., Luo, Y., Quan, Q., Wang, B., Xue, X. and Zhang, Y. “An autonomous task assignment and decision-making method for coverage path planning of multiple pesticide spraying UAVs,” *Comput. Electron. Agric.*, vol. 212 pp. 108128, Sep. 2023, doi: 10.1016/j.compag.2023.108128.

[8] Emran, B. and Najjaran, H. “A review of quadrotor: An underactuated mechanical system,” *Annu. Rev. Control*. vol. 46, pp. 165-180, 2018, doi: 10.1016/j.arcontrol.2018.10.009.

[9] Yang, S., Han, J., Xia, L. and Chen, Y. “Adaptive robust servo constraint tracking control for an underactuated quadrotor UAV with mismatched uncertainties,” *ISA Trans.*, vol. 106, pp. 12-30, Nov, 2020, doi: 10.1016/j.isatra.2020.07.007.

[10] Amin, R., Aijun, L. and Shamshirband, S. “A review of quadrotor UAV: control methodologies and performance evaluation,” *Int. J. Autom. Control*, vol. 10, pp. 87-103, May. 2016, doi: 10.1504/IJAAC.2016.076453.

[11] Zhao, Z. and Jin, X. “Adaptive neural network-based sliding mode tracking control for agricultural quadrotor with variable payload,” *Comput. Electr. Eng.*, vol. 103, pp. 108336, Oct. 2022, doi: 10.1016/j.compeleceng.2022.108336.

[12] Camci, E., Kripalani, D., Ma, L., Kayacan, E. and Khanesar, M. “An aerial robot for rice farm quality inspection with type-2 fuzzy neural networks tuned by particle swarm optimization-sliding mode control hybrid algorithm,” *Swarm Evol. Comput.*, vol. 41, pp. 1-8, Aug. 2018, doi: 10.1016/j.swevo.2017.10.003.

[13] Weng, F., Wei, H., Huang, Y. and Hou, L. "Trajectory tracking control for uncertain agricultural quadrotor based on combining ASMC and NFTSMC," *Int. J. Autom. Control*, vol. 17, pp. 635-656, Aug. 2023, doi: 10.1504/IJAAC.2023.134559.
[14] Abdelkader, M., Güler, S., Jaleel, H. and Shamma, J. "Aerial swarms: Recent applications and challenges," *Curr. Robot. Rep.*, vol. 2, pp. 309-320, Jul. 2021, doi: 10.1007/s43154-021-00063-4.
[15] L. F. C. Ccari, P. R. Yanyachi, "A novel neural network-based robust adaptive formation control for cooperative transport of a payload using two underactuated quadrotors," *IEEE Access*, vol. 11, pp. 36015-36028, Apr. 2023, doi: 10.1109/ACCESS.2023.3265957.
[16] Su, Y., Bhowmick, P. and Lanzon, A. "A robust adaptive formation control methodology for networked multi-UAV systems with applications to cooperative payload transportation," *Control Eng. Pract.*, vol. 138, pp. 105608, Sep. 2023, doi: 10.1016/j.conengprac.2023.105608.
[17] Miao, Q., Zhang, K. and Jiang, B. "Fixed-Time Collision-Free Fault-Tolerant Formation Control of Multi-UAVs Under Actuator Faults," *IEEE Trans. Cybern*, vol. 54, pp. 3679-3691, Jun. 2024, doi: 10.1109/TCYB.2024.3352251.
[18] Elmokadem, T. "Distributed coverage control of quadrotor multi-UAV systems for precision agriculture," *IFAC-PapersOnLine*, vol. 52, pp. 251-256, 2019, doi: 10.1016/j.ifacol.2019.12.530.
[19] Hegde, A. and Ghose, D. "Multi-UAV distributed control for load transportation in precision agriculture," *AIAA Scitech 2020 Forum*, pp. 2068, Jan 2020, doi: 10.2514/6.2020-2068.
[20] Ju, C. and Son, H. "Multiple UAV systems for agricultural applications: Control, implementation, and evaluation," *Electronics*, vol. 7, pp. 162, Aug. 2018, doi: 10.3390/electronics7090162.
[21] L. F. C. Ccari, W. Aguilar, E. Supo, E. S. Espinoza, Y. S. Vidal, N. Medina, and L. Pari, "Robust finite-time adaptive nonlinear control system for an EOD robotic manipulator: Design, implementation, and experimental validation," *IEEE Access*, vol. 12, pp. 93859-93875, Jul. 2024, doi: 10.1109/ACCESS.2024.3424463.
[22] L. F. C. Ccari, P. R. Yanyachi, J. C. Cutipa Luque, and D. Yanyachi, "Distributed robust adaptive control for finite-time flight formation of multi-quadrotor systems with large lumped uncertainties," *IEEE Access*, vol. 12, pp. 113384-113405, Aug. 2024, doi: 10.1109/ACCESS.2024.3439414.
[23] Wu, J., Peng, H., Chen, Q. and Peng, X. "Modeling and control approach to a distinctive quadrotor helicopter," *ISA Trans.*, vol. 53, pp. 173-185, Jan. 2014, doi: 10.1016/j.isatra.2013.08.010.
[24] Huang, Y., Liu, W., Li, B., Yang, Y. and Xiao, B. "Finite-time formation tracking control with collision avoidance for quadrotor UAVs," *J. Frankl. Inst.*, vol. 357, pp. 4034-4058, May. 2020 doi: 10.1016/j.jfranklin.2020.01.014.
[25] Tripathi, V., Kamath, A., Behera, L., Verma, N. and Nahavandi, S. "An Adaptive Fast Terminal Sliding-Mode Controller With Power Rate Proportional Reaching Law for Quadrotor Position and Altitude Tracking," *IEEE Trans. Syst., Man, Cybern.: Syst.*, vol 52, pp. 3612-3625, Apr. 2021, doi: 10.1109/TSMC.2021.3072099.
[26] Yanyachi, P. and Espinoza-García, B. "UAV's Applications for row and field crop Phenotyping and Mapping in Majes-Arequipa," *2021 IEEE Int. Conf. Aerosp. Signal Process. (INCAS)*, pp. 1-4, 2021, doi: 10.1109/INCAS53599.2021.9666918.

Pablo Raul Yanyachi (Senior Member, IEEE) received the Master of Science degree in automatic control from the Polytechnic Institute of Leningrad, and the Ph.D. degree in electrical engineering from the Polytechnic School, University of São Paulo, Brazil. He is currently a Main Professor of the Academic Department of Electronic Engineering, National University of San Agustín Arequipa (UNSA). He is a Station Manager of Nasa Laser Tracking Station TLRS-3, Arequipa, Peru. He is also the Director of the Instituto de Investigación Astronómico y Aeroespacial Pedro Paulet (IAAPP), UNSA.

Luis F. Canaza Ccari received a B.Sc. degree in Electronic Engineering from the National University of San Agustin of Arequipa (UNSA), Peru, in 2021. He is a RENACYT researcher currently working as a Research Assistant at the Pedro Paulet Aerospace and Astronomy Research Institute (IAAPP) - UNSA. His research interests include autonomous robotics, advanced control, and system modeling applied to quadcopters, robotic manipulators, and multi-agent systems.

Daniel Yanyachi received the M.Sc. and Ph.D. degrees in electrical engineering from the Leningrad Polytechnic Institute. He has lectured for many years as a Full Professor with the Electronic Engineering Department, Universidad Nacional de San Agustín de Arequipa, Peru. His research interests include processing control systems, mining, manufacturing, and complex and advanced control systems.